Partial Volume Corrections for Tau and Amyloid PET Imaging with [18F]THK5351 and [11C]PiB

著者	Shidahara M., Thomas A.B., Okamura N., Ibaraki M., Matsubara K., Oyama S., Ishikawa Y., Watanuki S., Iwata R., Furumoto S., Yanai K., Watabe H., Tashiro M.
journal or publication title	CYRIC annual report
volume	2016-2017
page range	142-146
year	2017
URL	http://hdl.handle.net/10097/00128080

VII. 4. Partial Volume Corrections for Tau and Amyloid PET Imaging with [^{18}F]THK5351 and [^{11}C]PiB

Shidahara M.[1,2], Thomas A.B.[3], Okamura N.[4], Ibaraki M.[5], Matsubara K.[5], Oyama S.[2], Ishikawa Y.[2], Watanuki S.[2], Iwata R.[2], Furumoto S.[2], Yanai K.[6], Watabe H.[2], and Tashiro M.[2]

[1]*Department of Quantum Science and Energy Engineering, Tohoku University*
[2]*Cyclotron Radioisotope Center, Tohoku University*
[3]*Institute of Nuclear Medicine, University College London*
[4]*Tohoku Medical and Pharmaceutical University*
[5]*Research Institute for Brain and Blood Vessels-Akita*
[6]*Department of Pharmacology, Tohoku University School of Medicine*

Introduction

Brain Positron Emission Tomography (PET) imaging of neurofibrillary tangle (tau) and amyloid β peptide (amyloid) has been recognized as having an important role in the diagnosis of Alzheimer's disease (AD)[1)]. However, due to the spatial resolution of PET system, the PET image suffers from partial volume effect (PVE), where regional uptake of radiotracer is blurred and its quantification is degraded[2)]. In order to compensate PVE on observed brain PET images, many partial volume correction (PVC) methods, which utilize both the spatial resolution and individual structural images (e.g. MRI), have been proposed. The classical and popular PVC methods are Müller-Gärtner (MG)[3)] and the geometric transfer matrix (GTM) methods[4)].

There have been several reports which state that applying PVC improved image quality of tau and amyloid PET and improved the accuracy and precision of the quantification of tracer uptake[5-14)]. However, in many cases, the applied PVC method were limited to MG or GTM. Furthermore, Greve et al. reported that different PVC methods (MG, GTM, and Meltzer) result in different conclusions in a FDG cross-sectional aging study of elderly subjects[15)]. There is a need to perform a comparison study of the popular PVC methods for tau and amyloid PET studies and to explore the possibility of other techniques. In this study, we report 4 PVC methods for tau and amyloid PET images: traditional MG, GTM, and other Regional voxel-based (RBV)[16)] and Iterative Yang (IY)[17)] methods.

Material and Methods

PET and MR images of 1 HC (81 y.o., Female) and 1 AD (80 y.o., Male) subjects, who had both a [^{11}C]PiB and [^{18}F]THK5351 PET scan, were used in this study. The PET studies were performed using Eminence STARGATE (Shimadzu Inc., Kyoto, Japan). After a 10-min ^{131}Cs transmission scan, 60- and 70-min dynamic scanning was started immediately after the intravenous administration of 304.9-347.4 MBq [^{11}C]PiB and 176.1-178.0 MBq [^{18}F]THK5351, respectively. All emission data were reconstructed using 3D-DRAMA (1 iteration, 128 filter cycle, 30 relaxation factor)[18] with attenuation and scatter corrections[19] and post filter of three dimensional Gaussian (3 mm FWHM). SUV images with 40-60 min time frame images were obtained. This study was approved by the Ethics Committee on Clinical Investigations of Tohoku University School of Medicine, and was performed in accordance with the Declaration of Helsinki. Written informed consent was obtained from all subjects after a complete description of the study had been made.

Brief explanations of 4 PVC methods were described below by using abbreviations as shown in Table 1. The MG[3] is voxel-based method for gray matter regions with the assumption of uniform-tracer uptake in white matter.

$$f_{c,gray}(x) = \frac{f(x) - A_{white,f(x)} \cdot p_{white}(x) \otimes PSF}{p_{gray}(x) \otimes PSF}, \tag{1}$$

The GTM method[4, 20] is ROI-based method and $C_{i,f(x)}$ is calculated as follows,

$$\begin{bmatrix} C_{1,f(x)} \\ \vdots \\ C_{i,f(x)} \\ \vdots \\ C_{N,f(x)} \end{bmatrix} = \mathbf{T}^{-1} \begin{bmatrix} A_{1,f(x)} \\ \vdots \\ A_{i,f(x)} \\ \vdots \\ A_{N,f(x)} \end{bmatrix}, \tag{2}$$

where **T** is the geometric transfer matrix of t_{ij}, which represents the contribution of spill-over from D_i into D_j. The RBV is an extension of the GTM and the voxel-wise correction of Yang et al.[21]. This process is given below:

$$\begin{aligned} f_c(x) &= f(x) \cdot \left[\frac{f_s(x)}{f_s(x) \otimes PSF} \right] \\ f_s(x) &= \sum_{i=1}^{N} \left[C_{i,f(x)} \cdot p_i(x) \right] \end{aligned} . \tag{4}$$

The Iterative Yang (IY) is a further adaptation of the Yang method[21]. This process is iterated several times with iteration number k is given below:

$$
\begin{aligned}
f_c^0(x) &= f(x) \\
f_c^{k+1}(x) &= f(x) \cdot \left[\frac{f_s^k(x)}{f_s^k(x) \otimes PSF} \right] \\
f_s^k(x) &= \sum_{i=1}^{N} \left[A_{i, f_c^k(x)} \cdot p_i(x) \right]
\end{aligned}
\tag{5}
$$

Automated parcellation of individual MR image was implemented by the FreeSurfer neuroimage analysis software package with version 5.1. The assignment of the parcellation map into 50 regions is shown in previous our report[22]. PVC processes were implemented using the PETPVC toolbox (https://github.com/UCL/PETPVC) and were applied assuming a resolution of 5 mm FWHM. Both uncorrected and PVC images with [^{18}F]THK5351 and [^{11}C]PiB were normalized with averaged ROI value in cerebellar grey matter to generate SUVR images.

Results and discussion

Figure 1 shows SUVR values of uncorrected PET images, 3 voxel-based and 1 ROI-based PVC results of the HC and AD subjects, for both tracers. The amount of recovery by RBV and IY were almost the same, similar with that of GTM, but different from those of MG (e.g., hippocampus of AD in [^{18}F]THK5351 and frontal of AD in [^{11}C]PiB). For HC subject, MG showed small increase of tracer uptake compared with other methods.

In the present study, we compared 4 partial volume correction methods for tau and amyloid PET imaging. Subjects undergoing tau and amyloid PET imaging are often expected to have brain atrophy, with or without physiological change in the region. It is difficult to accurately quantify tracer uptake in atrophic regions due to PVE. PVC for tau and amyloid PET imaging is expected to compensate PVE for more accurate quantification of tracer uptake, and is therefore essential for these applications[8].

However, the presented results suggest that most PVC techniques can produce different amounts of recovery in each region, subject condition, and tracer, even though RBV and IY showed the same results. In particular, MG showed different amount of recovery between subject conditions. In a previous study by Thomas et al., after PVC of MG, overestimation of [^{11}C]PiB uptake in the hippocampal region of an AD phantom was observed, even though that of a HC phantom was not[16]. We also observed a similar tendency with this correction technique. This indicates that tracer uptake in the hippocampal region after MG PVC may lead to a misinterpretation of pathological change.

Conclusion

PVC is essential processing when studying populations that are likely to have atrophy. However, in regions of high uptake of [^{18}F]THK5351 and [^{11}C]PiB, different PVCs demonstrated different SUVRs. The degree of difference between PVE uncorrected and corrected data depends on not only PVC algorithm but also subject conditions. Traditional PVC methods are straight-forward to implement but careful interpretation of the results is necessary.

References

1) Okamura N, Harada R, et al. *Ageing Res Rev*. (2016) 107-13.
2) Soret M, Bacharach SL, et al. *J Nucl Med*. **48** (2007) 932-45.
3) Muller-Gartner HW, Links JM, et al. *J Cereb Blood Flow Metab*. **12** (1992) 571-83.
4) Rousset OG, Ma Y, et al. *Journal of nuclear medicine*. **39** (1998) 904-11.
5) Adamczuk K, De Weer AS, et al. *Neuroimage Clin*. **2** (2013) 512-20.
6) Brendel M, Hogenauer M, et al. *Neuroimage*. **108** (2015) 450-9.
7) Forster S, Yousefi BH, et al. *Eur J Nucl Med Mol Imaging*. **39** (2012) 1927-36.
8) Ito H, Shinotoh H, et al. *Eur J Nucl Med Mol Imaging*. **41** (2014) 745-54.
9) Matsubara K, Ibaraki M, et al. *Neuroimage*. **143** (2016) 316-24.
10) Mori T, Shimada H, et al. *J Neurol Neurosurg Psychiatry*. **85** (2014) 449-55.
11) Rullmann M, Dukart J, et al. *J Nucl Med*. **57** (2016) 198-203.
12) Scholl M, Lockhart SN, et al. *Neuron*. **89** (2016) 971-82.
13) Su Y, Blazey TM, et al. *Neuroimage*. **107** (2015) 55-64.
14) Villemagne VL, Furumoto S, et al. *Eur J Nucl Med Mol Imaging*. **41** (2014) 816-26.
15) Greve DN, Salat DH, et al. *Neuroimage*. **132** (2016) 334-43.
16) Thomas BA, Erlandsson K, et al. *Eur J Nucl Med Mol Imaging*. **38** (2011) 1104-19.
17) Erlandsson K, Buvat I, et al. *Phys Med Biol*. **57** (2012) R119-59.
18) Tanaka E, Kudo H. *Phys Med Biol*. **55** (2010) 2917-39.
19) Ibaraki M, Matsubara K, et al. *Ann Nucl Med*. **30** (2016) 690-8.
20) Rousset OG, Collins DL, et al. *Journal of nuclear medicine*. **49** (2008) 1097-106.
21) Yang C, Huanf C, et al. *IEEE Trans Nucl Sci*. **43** (1996) 3322-7.
22) Shidahara M, Thomas BA, et al. *Ann Nucl Med*. **31** (2017) 563-9.

Table 1. Definitions and abbreviations for PVC processing

Abbreviation	Description
$f(x)$	uncorrected PET image
$f_c(x)$	PVE corrected PET image
$f_s(x)$	synthetic PET image
$p_i(x)$	anatomical probability of *i*-th region at location x
N	the total number of regions
$A_{i, f(x)}$	Averaged value of $f(x)$ at i-th region
$C_{i, f(x)}$	PVE corrected value for $f(x)$ at i-th region
D_i	Volume of i-th region
PSF	Point spread function
$\otimes$	Operation of three-dimensional convolution integral.

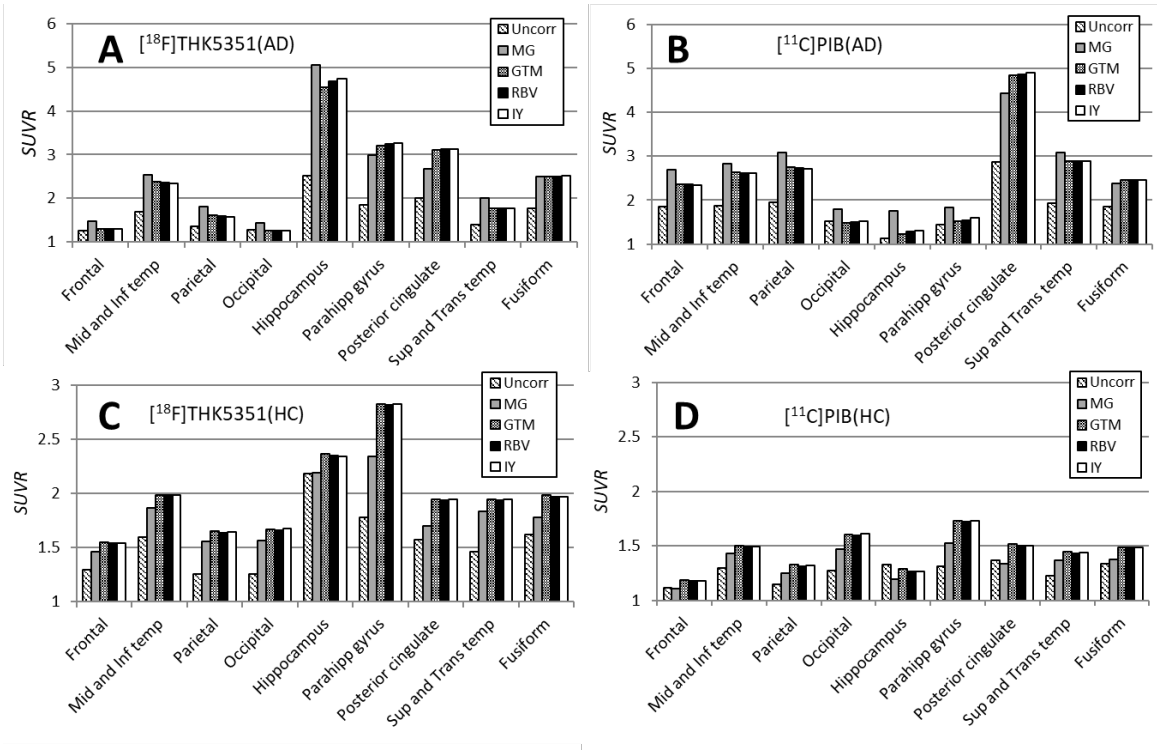

Figure 1. ROI comparisons of uncorrected and PVC SUVRs for a HC and AD subject with [^{18}F]THK5351 and [^{11}C]PiB